Design and optimization of a longitudinal feedback kicker cavity for the HLS-Ⅱ storage ring*

XU Wei(徐卫)[1,2;1)] W. Z. Wu[2] HE Duo-Hui(何多慧)[1] Y. K. Wu[2;2)]

[1] National Synchrotron Radiation Laboratory (NSRL), University of Science and Technology of China, Hefei 230029, China
[2] Department of Physics, Duke University, Durham, NC 27708-0319, USA

Abstract: In the Hefei Light Source (HLS) storage ring, multibunch operation is used to obtain a high luminosity. Multibunch instabilities can severely limit light source performance with a variety of negative impacts, including beam loss, low injection efficiency, and overall degradation of the beam quality. Instabilities of a multibunch beam can be mitigated using certain techniques including increasing natural damping (operating at a higher energy), lowering the beam current, and increasing Landau damping. However, these methods are not adequate to stabilize a multibunch electron beam at a low energy and with a high current. In order to combat beam instabilities in the HLS storage ring, active feedback systems including a longitudinal feedback system (LFB) and a transverse feedback system (TFB) will be developed as part of the HLS upgrade project, the HLS-Ⅱ storage ring project. As a key component of the longitudinal bunch-by-bunch feedback system, an LFB kicker cavity with a wide bandwidth and high shunt impedance is required. In this paper we report our work on the design of the LFB kicker cavity for the HLS-Ⅱ storage ring and present the new tuning and optimization techniques developed in designing this high performance LFB kicker.

Key words: longitudinal feedback system, kicker, nose cone

PACS: 29.20.db, 29.27.Bd **DOI:** 10.1088/1674-1137/37/3/037003

1 Introduction

The Hefei Light Source (HLS) is currently undergoing a major upgrade which will greatly improve its performance [1]. In order to maintain a highly stable electron beam in the storage ring with a high current, active feedback systems, both longitudinal and transverse, are required to help suppress the coupled bunch instabilities (CBIs) [2]. A bunch-by-bunch electron beam feedback system is composed of three subsystems. The first one is the signal detection system which picks up the bunch signal using a beam position monitor (BPM) and generates the bunch phase signal using the front-end processing unit. The second system, the digital signal processing system, which is implemented using digital signal processors (DSPs) or a field-programmable gate array (FPGA), processes the bunch signal and computes the correction signal for each bunch. The third system is the actuator in which the correction signal is first amplified by an RF power amplifier and then applied to the electron beam through a feedback kicker [3, 4]. In this work, our focus is the development of a longitudinal bunch-by-bunch feedback system for the HLS-Ⅱ storage ring.

The basic physical design of a longitudinal feedback kicker for the HLS-Ⅱ storage ring was presented in a previous paper [5]. This LFB kicker is a DAΦNE type LFB kicker with two ridged waveguides on each side of a pillbox cavity [6]. The kicker has two input ports and two output ports specially arranged so that the input ports and output ports are azimuthally separated by 90°. Since the cross-section shape of the vacuum chamber of the storage ring is an octagon, the design of the kicker cavity is realized in two steps. We first design an LFB kicker cavity with round beam pipes at both ends. Later, the design of the kicker cavity is retuned with a set of specially designed beam pipes to allow smooth transition from a round cross-section to an octagonal cross-section. The preliminary design with round beam pipes is used to determine the dependency between the kicker performance and kicker geometric parameters. The final design of the LFB kicker with transition parts is optimized with the Newton's method using the dependency obtained from the preliminary design.

The performance of the LFB kicker cavity can be enhanced by using nose cones. In this paper, we first discuss the effect of using nose cones, in particular, its

Received 25 April 2012

∗ Supported by National Natural Science Foundation of China (10979045, 11175182, 11175180)

1) E-mail: davidxu@mail.ustc.edu.cn

2) E-mail: wu@fel.duke.edu

impact on the resonant frequency and the shunt impedance. Next, we report the method of using the dependency relations between the cavity performance and geometric parameters to find the optimal design for the kicker cavity with round beam pipes. Finally we present the process of tuning the final design of the LFB kicker with transition beam pipes using the same dependency relations.

2 The effect of using nose cones

For a typical RF cavity built for accelerators, special tuners are usually used to fine tune its performance by inserting the tuner heads into the cavity. The tuning or optimization of the cavity performance can also be realized using some fixed addons inside the RF cavity. A nose cone is such an addon which can be used conveniently to alter the RF performance parameters without changing the main structure of the cavity. In the design of an LFB kicker cavity, the nose cones are introduced to improve the shunt impedance of the cavity, as used in the PLS LFB kicker and Duke LFB kicker [7, 8], and provide a means of shifting the resonant frequency in optimizing the cavity design.

2.1 Shunt impedance with nose cones

The LFB kicker cavity for the HLS-Ⅱ storage ring employs nose cones. Fig. 1 shows the schematic of a pillbox cavity with nose cones and one of the nose cones in the LFB kicker. The nose cone is a half torus attached to the entrance and exit of the beam pipes which are connected to the pillbox. The radius of the torus tube is 6 mm. The nose cones can increase the efficiency of energy gain by charged particles passing through the cavity by concentrating the electric field inside the kicker cavity and reduce its leakage to the adjacent beam pipes.

The energy gain of a relativistic particle passing through the LFB kicker with charge q is

$$\Delta E=qV_0T, \tag{1}$$

where V_0 is the gap voltage of the cavity and T is the transient time factor. The transient time factor can be calculated as

$$T=\frac{\int_0^l E_z\cos\left(\frac{\omega}{c}z\right)\mathrm{d}z}{\int_0^l E_z\mathrm{d}z}=\frac{\sin\left(\frac{\omega}{c}l_{\mathrm{eff}}\right)}{\frac{\omega}{c}l_{\mathrm{eff}}}, \tag{2}$$

where l_{eff} is the effective accelerating gap or the effective cavity length [9]. After the nose cones are attached to the inside of the pillbox, the path of the particles traversing the cavity does not change but the effective accelerating gap is reduced. This leads to an increase of the transient time factor from $T=0.70$ without nose cones to $T=0.73$ with nose cones for the HLS LFB kicker. The increase of the transient time factor is consistent with the observed

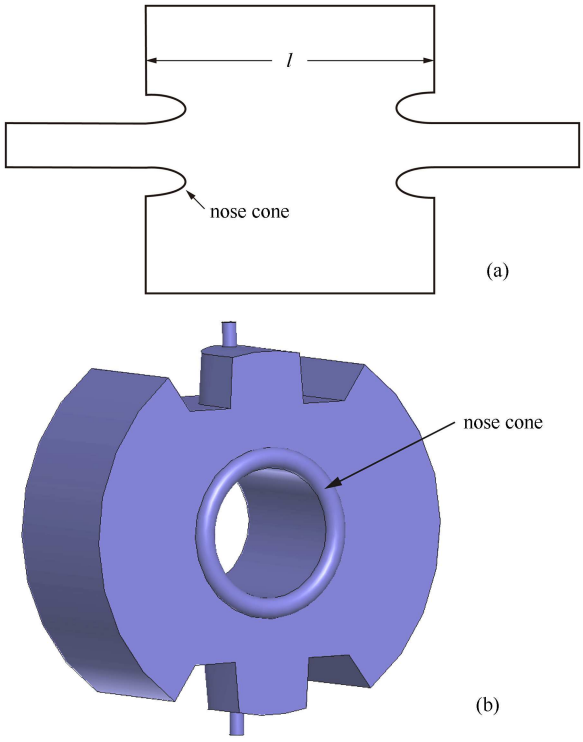

Fig. 1. The RF cavity with nose cones. (a) A 2D schematic of a pillbox cavity with nose cones. l is the gap of the pillbox. (b)The nose cone in the LFB kicker cavity for the HLS-Ⅱ storage ring.

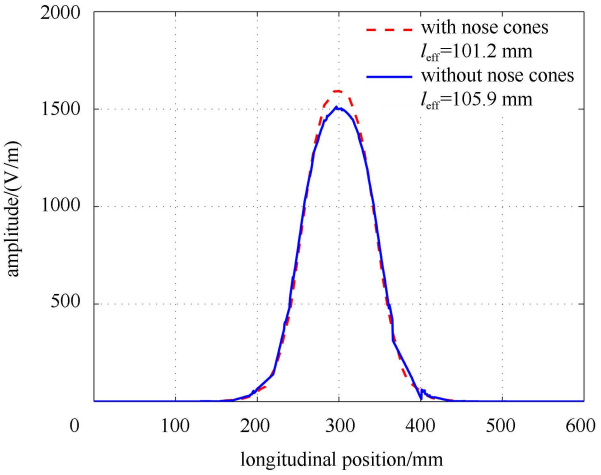

Fig. 2. The simulated electric fields along the beam axis of the LFB kicker. With nose cones, assuming the same input power, the electric field has larger amplitude inside the pillbox cavity and the cavity effective length is reduced from 105.9 mm (without nose cones) to 101.2 mm (with nose cones).

reduction of the effective cavity length from 105.9 mm (without nose cones) to 101.2 mm (with nose cones), a reduction of 4.4% (see Fig. 2).

In addition, the calculated shunt impedance is increased by 11% from 1561 Ω (without nose cones) to 1740 Ω (with nose cones). This is the direct evidence that nose cones help to improve the efficiency of providing acceleration to charged particles.

2.2 Cavity perturbation

During the operation of an RF cavity with beams, the cavity performance, especially the resonant frequency, may change from time to time due to various reasons, e.g. the deformation caused by the change of temperature. In order to make the cavity work properly we need to tune the cavity. This is often done by inserting a metallic piston (a tuner) into the cavity. It is useful to predict the effect of such modifications to the cavity performance. If the tuning is small, i.e., the original fields do not change significantly after the modification, the cavity can be analyzed using the perturbation method. There are two kinds of cavity perturbations. The material perturbation treats the small change in the permittivity or permeability of all or part of the material filling in the cavity. The shape perturbation treats the small changes of the cavity shape or volume which can be accomplished by using a tuner.

The nose cones in the LFB kicker change the volume of the cavity so a frequency change is expected. This change can be analyzed using the shape perturbation method. Unlike the RF tuners which can be used to provide tuning of the cavity dynamically during its operation, the nose cone is useful in the design stage to fine-tune the cavity resonant frequency.

The perturbation method can be used to predict the change of the resonant frequency. Let us consider a cavity with an arbitrary shape and a volume V_0. The material filling in the cavity has the permittivity of ϵ and permeability of μ. The original fields in the cavity are $\bar{E}_0$ and $\bar{H}_0$, and the resonant frequency of the cavity is ω_0. After perturbation, the resonant frequency becomes ω. Suppose that the volume of the cavity is reduced by ΔV which is part of the original volume, and ΔV is small enough, the fields after the perturbation can be represented using the original fields. The fractional change in resonant frequency can be approximated as [10]

$$\frac{\omega-\omega_0}{\omega_0}\simeq\frac{\int_{\Delta V}\left(\mu\left|\bar{H}_0\right|^2-\varepsilon\left|\bar{E}_0\right|^2\right)\mathrm{d}V}{\int_{V_0}\left(\epsilon\left|\bar{E}_0\right|^2+\mu\left|\bar{H}_0\right|^2\right)\mathrm{d}V}. \tag{3}$$

This formula can be expressed in the form of the electric and magnetic energies stored in the cavity

$$\frac{\Delta\omega}{\omega_0}\simeq\frac{\Delta W_\mathrm{m}-\Delta W_\mathrm{e}}{W_0}, \tag{4}$$

where ΔW_m and ΔW_e are the magnetic and electric energy stored in ΔV, respectively. This result shows that the resonant frequency change due to the perturbation depends on the difference between the magnetic energy and electric energy in volume ΔV.

In the LFB kicker, the nose cones are small enough compared with the cavity itself. Therefore, we can assume that the electromagnetic fields in the area of the nose cone are constant and can be represented by the fields at the center of the torus tube before perturbation. The distance between the center of the tube and the center of the torus is $R'=44$ mm. The field components of the fundamental mode of an ideal pillbox cavity can be written as (assuming that the cavity is under vacuum):

$$E_z(r,t) = E_0J_0\Big(\frac{\nu_{01}}{a}r\Big)\cos(\omega t), \tag{5}$$

$$H_\phi(r,t) = -\frac{E_0}{\eta}J_1\Big(\frac{\nu_{01}}{a}r\Big)\sin(\omega t), \tag{6}$$

$$E_r = E_\phi=H_r=H_z=0, \tag{7}$$

where a is the radius of the pillbox, η is the wave impedance and $\omega=c\nu_{01}/a\sqrt{\epsilon_r\mu_r}$ is the resonant frequency of the pillbox cavity, c is the speed of light, and ν_{01} is the first root of Bessel function $J_0(x)$. Using Eqs. (5) and (6), we find the amplitude of the fields in the location of the nose cone:

$$|E_z(R')|=E_0J_0\Big(\frac{\nu_{01}}{a}R'\Big), \tag{8}$$

$$|H_\phi(R')|=\frac{E_0}{\eta_0}J_1\Big(\frac{\nu_{01}}{a}R'\Big), \tag{9}$$

where $\eta_0=\sqrt{\mu_0/\epsilon_0}=377\ \Omega$ is the wave impedance in free-space. Using these fields the difference of the energy changes in the magnetic and electric forms is

$$\begin{aligned}\Delta W_\mathrm{m}-\Delta W_\mathrm{e} &= \frac{1}{4}\Delta V\left(\mu_0|H_\phi(R')|^2-\epsilon_0|E_z(R')|^2\right)\\ &= \frac{\Delta V}{4}\epsilon_0\Big(J_1^2\Big(\frac{\nu_{01}}{a}R'\Big)-J_0^2\Big(\frac{\nu_{01}}{a}R'\Big)\Big).\end{aligned} \tag{10}$$

With the geometric parameters of the LFB kicker, we have $\Delta W_\mathrm{m}-\Delta W_\mathrm{e}=-0.12\epsilon_0E_0^2\Delta V$. The volume of these two nose cones is 6.25×10^{-5} m^3 so we have $\Delta W_\mathrm{m}-\Delta W_\mathrm{e}=-7.50\times10^{-6}\epsilon_0E_0^2$. The "−" sign indicates a reduction of the resonant frequency by attaching the nose cones and this frequency decrement is proportional to the volume of the nose cones.

With the electric field in Eq. (5), the total energy can

be calculated as follows:

$$\begin{aligned} W_0 &= W_{\rm m}+W_{\rm e}=2W_{\rm e} \\ &= \frac{1}{2}E_0^2\epsilon_0\int_0^l {\rm d}z\int_0^{2\pi}{\rm d}\phi\int_0^a J_0^2\Big(\frac{\nu_{01}}{a}r\Big)r{\rm d}r \\ &= \frac{\pi}{2}\epsilon_0 l a^2 J_1^2(\nu_{01})E_0^2. \end{aligned}$$

For the HLS LFB cavity, we have $W_0 = 3.3\times10^{-4}\epsilon_0 E_0^2$. Therefore, the projected fractional change of the resonant frequency is $\Delta\omega/\omega \simeq -2.3\%$. In order to compensate for this reduction of the resonant frequency, we need to reduce the radius of the pillbox by 2.3% accordingly. This is good because it makes the LFB kicker somewhat more compact by shrinking its size.

We can also calculate the central (or resonant) frequency change with a fixed cavity geometry using the simulation method. The resonant frequency of the LFB kicker is reduced from 1000 MHz (without nose cones) to 971.7 MHz (with nose cones), a reduction of 2.8% in frequency. This is rather consistent with the result from the estimate (-2.3%) using an ideal pillbox cavity.

3 Dependency calculation for LFB kicker cavity

Although an RF cavity can be tuned using tuners after it is made, the use of tuners greatly increases the complexity of the cavity. Furthermore, the tuners can only provide a limited tuning of the cavity performance. In order to obtain an LFB cavity with specific performance, we need to tune the main structure of the cavity during the design process. The LFB kicker cavity has a complicated structure which consists of many geometric parameters. To allow optimization of the kicker cavity design, it is very useful to develop dependency relations between the cavity performance parameters and a set of cavity geometric parameters. To simplify this process, we have carefully chosen several important geometric parameters for the dependency calculation. The Duke LFB kicker is used as the starting point for the calculation [8]. Some geometric parameters are fixed such as the beam pipe radius and the pillbox gap. Some geometric parameters do not have much flexibility due to the space limitation such as the cavity length. Finally the three geometric parameters which are selected to calculate the dependency are R_1, R_2 and g, shown in Fig. 3. R_1 is the pillbox radius which directly determines the resonant frequency of the kicker. R_2 and g are the main geometric parameters of the ridged waveguide which determine the inductance and capacitance, i.e., the input impedance of the waveguide [11]. So these two parameters affect the coupling factor between the input and output coaxial lines and the ridged waveguides. To save the computation time, only a quarter structure of the kicker is simulated during the dependency calculation because the boundary condition of the kicker cavity and the electromagnetic fields are symmetric. In fact for the $\rm TM_{010}$ mode of an ideal pillbox cavity, the electric fields are tangential and the magnetic fields are perpendicular to the symmetry planes of the kicker cavity. This allows us to assign a perfect magnetic conductor surface at these symmetry planes.

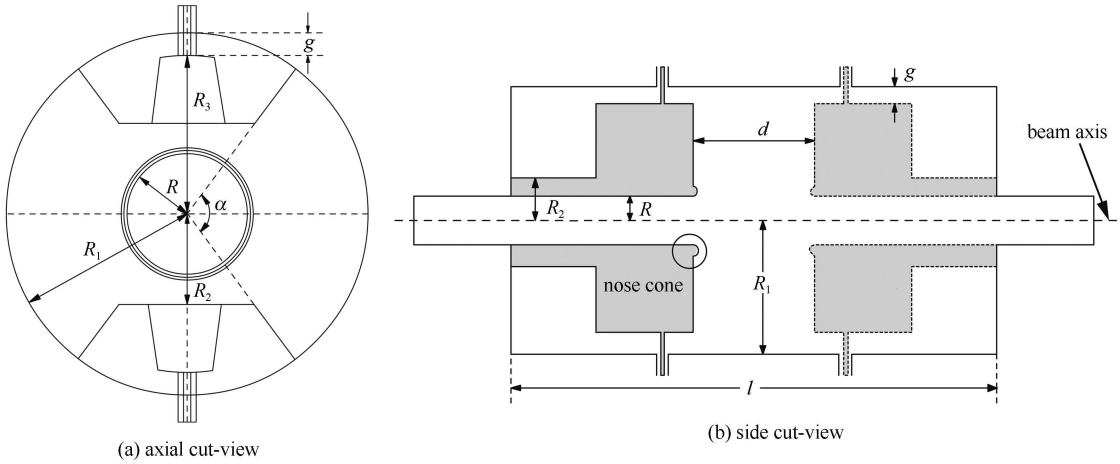

Fig. 3. The cross-sections of the LFB kicker cavity model. Important geometric parameters include the following: the radius of the beam pipe R is 38 mm, R_1 is the pillbox radius, R_2 is the height of the back cavity and R_3 is the ridge height, d is the pillbox gap and g is the waveguide gap, α is the angle between the waveguide barriers and l is the cavity length excluding the outer beam pipes. The input and output ports are not in the same plane. The dashed part in the side cut-view indicates a rotation of 90° along the direction of the beam pipes.

After simulating a set of the LFB kicker structures with different geometric parameters, we obtain the dependent relations of a set of key performance parameters, such as the central frequency ($f_{\rm cf}$), the cavity bandwidth (BW), the shunt impedance ($R_{\rm s}$) and the geometric parameters (R_1, R_2, g). Fig. 4 shows the dependency of the kicker central frequency. The $f_{\rm cf}$ dependency curves are grouped into 4 sets by different values of R_1. With a larger R_1, we have lower central frequencies. This is reasonable because the resonant frequency of $\rm TM_{010}$ mode is inversely proportional to the pillbox radius. If the central frequencies located within 969±5 MHz are considered as good results, we have many solutions that satisfy this design goal. Fig. 5 shows the dependency of the kicker bandwidth (BW). The BW dependency curves are grouped into 3 sets using different values of R_2. Bandwidths are locally maximized when the waveguide gap is in the range of 8 mm to 10 mm. A set of solutions with the bandwidth higher than 102 MHz are found through the bandwidth dependency calculation. Among these solutions, two solutions satisfy both central frequency and bandwidth requirements, which are (R_1, R_2, g) = (115 mm, 74 mm, 9 mm) and (115 mm, 68 mm, 10 mm). The corresponding performance parameters are ($f_{\rm cf}$, BW) = (971.4 MHz, 102.6 MHz) and (969.1 MHz, 109.5 MHz), respectively. Fig. 6 shows the dependency of the kicker shunt impedance. Comparing Fig. 5 with Fig. 6, we can see that the shunt impedance is almost inversely proportional to the bandwidth. This is reasonable because the shunt impedance for a waveguide overloaded pillbox cavity can be approximated as

$$R_{\rm s}\approx 2\frac{R}{Q}\cdot Q_{\rm L}=2\frac{R}{Q}\cdot\frac{f_{\rm cf}}{BW}, \tag{11}$$

where R/Q is the R over Q factor which depends only on the kicker geometry and $Q_{\rm L}$ is the loaded quality factor [6]. As expected, a wider bandwidth is usually accompanied with a decreased shunt impedance. The shunt impedances of these two solutions are 1793 Ω and 1699 Ω, respectively. The LFB kicker with the geometric parameters of (115 mm, 74 mm, 9 mm) is finally selected because it has adequately high shunt impedance and more importantly, a shorter waveguide gap, which makes the assembly of the RF feedthroughs easier.

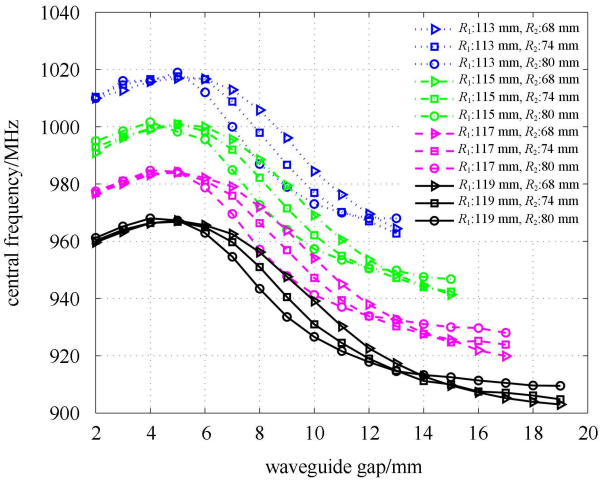

Fig. 4. The simulated central frequency dependency on the kicker geometric parameters.

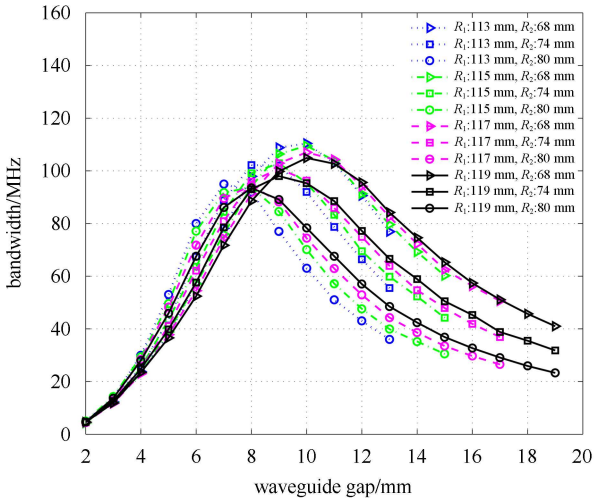

Fig. 5. The simulated bandwidth dependency on the kicker geometric parameters.

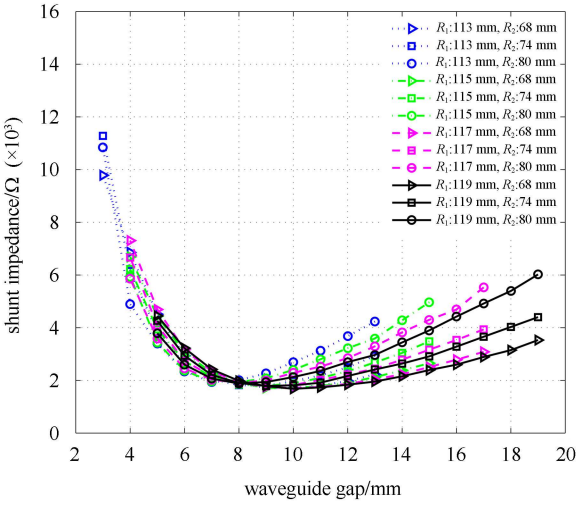

Fig. 6. The simulated shunt impedance dependency on the kicker geometric parameters.

4 Optimization of the LFB kicker with transition parts

The preliminary design of the LFB kicker with round beam pipes is obtained through the dependency calculation. In order to save time the calculation is carried

out using the quarter structure of the LFB kicker. After the transition part is added, we need to fine-tune the kicker to bring its performance back to our design specifications. We could do this by recalculating the cavity dependency as we do during the preliminary design. But the dependency calculation would take a lot of time even using a quarter kicker model. More importantly, the kicker with transition beam pipes is no longer symmetric so we would have to simulate the full kicker cavity.

Now we have three models of the LFB kicker with small differences, (1) the quarter structure of the kicker with round beam pipes, (2) the full structure of the kicker with round beam pipes, and (3) the full structure of the kicker with transition from round beam pipes to octagonal vacuum chambers. For the full LFB kicker model, the electric and magnetic fields could not be exactly the same as the quarter cavity model, an idealized cavity with imposed symmetry, especially when higher order modes are present. Therefore, the calculated kicker cavity performance parameters are slightly different between a quarter cavity model and a full cavity model. Some differences can be attributed to the underlining simulation model as the mesh structure changes when the full cavity is simulated. The difference between the preliminary design and the final design is the shape of the beam pipes. This difference of the boundary condition of the kicker can also causes small changes in the cavity performance even though the beam pipes are outside the pillbox cavity. Therefore, these three structures should have very similar performance. The simulation results confirm this. The main performance parameters of these three structures with the same geometric parameters are listed in Table 1.

Table 1. Main performance parameters (simulation results) of the LFB kicker with different structures.

parameter	quarter structure with round beam pipes	full structure with round beam pipes	kicker with transition from round to octagonal beam pipes
$f_{\rm cf}$/MHz	971.4	971.7	971.2
BW/MHz	102.7	100	100.1
$R_{\rm s}/\Omega$	1800	1740	1750

Nevertheless, the dependency relations computed using the quarter cavity model is still useful for the other two cavity models. This important observation is made as we realize that the difference in the electric and magnetic fields among the three models is small. Let us consider a performance parameter for two similar cavity models. This parameter can be expressed as functions $A(x)$ and $B(x)$ for these two models, with x being the geometric variable to be varied. If $|(A(x)-B(x))/A(x)|\ll 1$, then we expect, $\partial A/\partial x \backsimeq \partial B/\partial x$, as long as A and B are well behaved smooth functions with smooth slopes with respect to x. In this case if the dependency of the first model is known ($\partial A(x)/\partial x$), this dependency can be used to estimate the necessary changes of $B(x)$,

$$B(x_2)=B(x_1)+\frac{\partial A}{\partial x}(x_1)(x_2-x_1).$$

In fact, this is the idea used in the Newton's method to solve differential equations [12]. Therefore we can realize the final design of the kicker cavity with transition beam pipes by using the same dependencies calculated from the quarter kicker model with round beam pipes.

4.1 Fitting of the dependencies between the kicker geometry and performance

Before we start to use the dependencies, we need to express them in analytical forms. In the following, the dependency function is constructed for the kicker cavity resonant frequency (or the central frequency) and bandwidth. The shunt impedance is not optimized further as it is a less critical parameter, and it already has a large value more than adequate for this cavity. Since the dependency curves of the central frequency and bandwidth may not be linear, we can fit a second degree polynomial to the data that we obtained from the dependency calculation. The model function with three independent variables has 9 coefficients, which can be expressed as

$$\begin{aligned} f(x,y,z) \;=\; & a_0+a_1x+a_2y+a_3z+a_4x^2+a_5y^2 \\ & +a_6z^2+a_7xy+a_8xz+a_9yz, \end{aligned} \tag{12}$$

where x, y, and z represent the kicker geometric parameters R_1, R_2 and g, respectively. Each of the dependency curves ($f_{\rm cf}$, BW) has 36 data points; this means that the constrains for data fitting are more than the number of fitting parameters. A good fitting method for dealing with this overdetermined problem is the least square fitting. The method of least square finds the best fit by minimizing the sum of the squares of the difference between the fitted function and data.

The fitting result of the central frequency as a function of the pillbox radius ($x=R_1$), back cavity height ($y=R_2$) and the waveguide gap ($z=g$) is

$$\begin{aligned} f_{\rm cf}(x,y,z) \;=\; & 2736.75-14.75x-6.12y-34.71z \\ & +0.0167x^2-0.0014y^2+0.3375z^2+0.0331xy \\ & +0.0775xz+0.1427yz, \end{aligned} \tag{13}$$

where x, y, and z are in millimeters and the frequency

is in megahertz. The rms value of the squared residuals is 0.84 MHz. The residual associated with a data point refers to the difference between the observed value and fitted value provided by the model function. The relative error between the simulated central frequencies and the fitted values is only 8.7×10^{-4}. The polynomial function describes the central frequency dependency very well, as shown in Fig. 7.

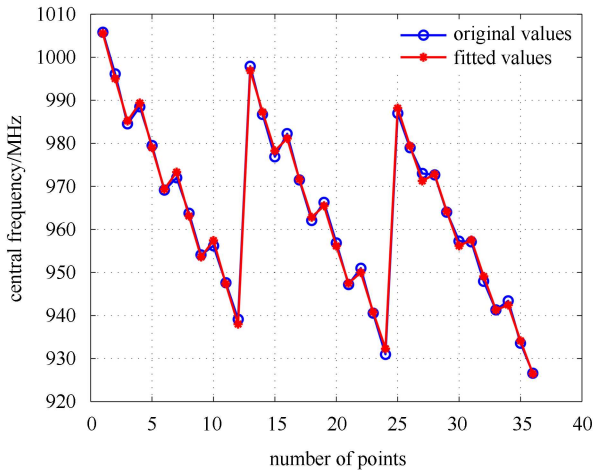

Fig. 7. Fitting results of the central frequency dependency.

The fitting result of the cavity bandwidth dependency is

$$\begin{aligned} f_{\rm bw}(x,y,z) = {} & -938.23+9.07x+5.61y+83.64z \\ & -0.1493x^2-0.1459y^2-3.7042z^2+0.2440xy \\ & +0.8225xz-1.5406yz, \end{aligned} \tag{14}$$

where $x=R_1$, $y=R_2$, and $z=g$ are also in millimeters and the bandwidth is in megahertz. We can see that the coefficients of the terms with z are larger than others. This means that the bandwidth is more sensitive to the waveguide gap than other geometric parameters. The rms value of the squared residuals is 1.34 MHz. Therefore, the relative error between the simulated bandwidths and the fitted ones is 1.4%. The fitting results are shown in Fig. 8.

4.2 Cavity tuning using Newton's method

We cannot directly use the solutions of Eqs. (13) and (14) to determine the kicker geometric parameters because the dependencies are based on the quarter structure of the LFB kicker with round beam pipes. A better way to do this is to use the iterative procedure to approach the solution step by step. In numerical analysis, the Newton's method is commonly used to find the approximations to the roots of a real-valued function [12]. The functions of the central frequency and bandwidth have three variables so we can fix one geometric parameter and find the solution using the other two parameters. Considering the assembly of the feedthroughs, the waveguide gap is fixed at 9 mm. The design requirements of the central frequency and the bandwidth are $\simeq$969 MHz and $\geqslant$102 MHz, respectively. The two functions we are going to solve are

$$\begin{aligned} f(x,y) &= f_{\rm cf}(x,y,9)-969, \\ g(x,y) &= f_{\rm bw}(x,y,9)-102. \end{aligned} \tag{15}$$

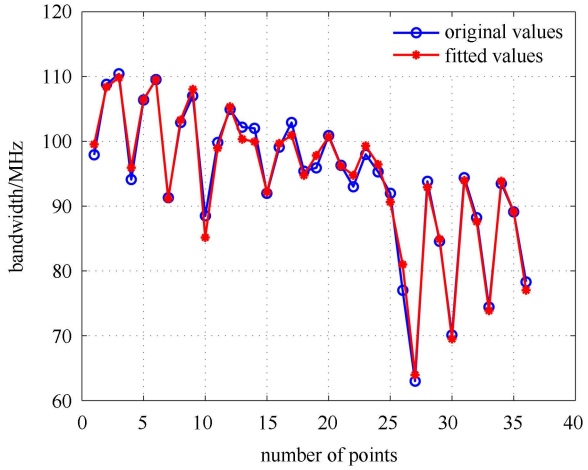

Fig. 8. Fitting results of the bandwidth dependency.

The Newton's method can be generalized to two or more dimensions. If we pick (x_0,y_0) as the initial guess, (x_1,y_1) is the next solution which will lead function f and g closer to zero:

$$\begin{aligned} f(x_1,y_1) = {} & f(x_0,y_0)+f_x(x_0,y_0)(x_1-x_0) \\ & +f_y(x_0,y_0)(y_1-y_0)\approx0, \\ g(x_1,y_1) = {} & g(x_0,y_0)+g_x(x_0,y_0)(x_1-x_0) \\ & +g_y(x_0,y_0)(y_1-y_0)\approx0, \end{aligned} \tag{16}$$

where $f_x=\partial f/\partial x$, $f_y=\partial f/\partial y$, $g_x=\partial g/\partial x$, $g_y=\partial g/\partial y$. (x_1,y_1) can be solved numerically if the slopes f_x, f_y, g_x, g_y are known at (x_0,y_0). With simple algebra we can find solutions for $f(x,y)=0$ and $g(x,y)=0$ using the following iteration procedure:

$$\begin{aligned} x_n &= x_{n-1}-\frac{f(x_{n-1},y_{n-1})g_y(x_{n-1},y_{n-1})-f_y(x_{n-1},y_{n-1})g(x_{n-1},y_{n-1})}{f_x(x_{n-1},y_{n-1})g_y(x_{n-1},y_{n-1})-f_y(x_{n-1},y_{n-1})g_x(x_{n-1},y_{n-1})}, \\ y_n &= y_{n-1}-\frac{f_x(x_{n-1},y_{n-1})g(x_{n-1},y_{n-1})-f(x_{n-1},y_{n-1})g_x(x_{n-1},y_{n-1})}{f_x(x_{n-1},y_{n-1})g_y(x_{n-1},y_{n-1})-f_y(x_{n-1},y_{n-1})g_x(x_{n-1},y_{n-1})}. \end{aligned} \tag{17}$$

Table 2. Iterative results for optimizing the LFB kicker cavity using Newton's method.

sequences	R_1/mm	R_2/mm	function values/MHz		simulated values/MHz	
			$f_{\rm cf}$	$f_{\rm bw}$	$f_{\rm cf}$	$f_{\rm bw}$
initial	115.0	74.0	971.60	100.10	971.2	100.1
1	115.4	73.0	969.75	102.53	970.0	101.6
2	115.6	72.7	968.56	102.88	967.9	100.7
3	115.6	71.7	969.77	104.00	970.2	102.6
4	115.8	71.6	968.32	103.98	969.2	102.8

The fitted functions cannot represent the dependency of the kicker performance very accurately because the dependency calculation is carried out using a different structure from the final design of the kicker cavity and the fitting itself has finite accuracy. To deal with these effects, for each step of iteration, the errors are computed using Eqs. (15) with the cavity central frequency and bandwidth obtained from cavity design simulation using the geometric parameters from the previous step. The simulation is implemented using the full kicker cavity with transition beam pipes. When evaluating Eq. (16), the slopes of functions f and g, i.e., f_x, f_y, g_x, g_y, are those from the fitted dependency results (Eqs. (13) and (14)) obtained using a quarter cavity model. The initial guess in our case is the geometric parameters of the preliminary design. The pillbox radius R_1 (x_0) is 115 mm and the back cavity height R_2 (y_0) is 74 mm. The initial central frequency and bandwidth are 971.2 MHz and 100.1 MHz, respectively which leads to $f(x_0,y_0)=2.2$ MHz and $g(x_0,y_0)=-1.9$ MHz according to Eqs. (15). The results for four consecutive iteration steps are listed in Table 2. After four iterations, a sufficiently accurate solution for R_1 and R_2 is obtained for the final design of the LFB kicker with transition beam pipes. Finally, we list the main performance parameters (simulated results) of the HLS-Ⅱ LFB kicker cavity in Table 3. This cavity has two specially designed transition beam pipes on the sides to allow a smooth vacuum transition from a round cross-section in the LFB cavity to an octagonal cross-section of the storage ring vacuum chambers.

4.3 Mechanical tolerance

The dependency relations can also be used to make specifications for the mechanical tolerance for certain critical geometric parameters. For R_1, R_2 and g, the mechanical tolerance is specified as ±0.12 mm. These tolerances are specified to make sure that the changes of the center frequency and bandwidth will be less than ±2 MHz and ±0.5 MHz, respectively, in the worst case scenario. These tolerances are reasonably easy to meet using modern computer numerical control (CNC) machines. If CNC machines are not available, these tolerance specifications can be further relaxed by a factor of two without significantly reducing the performance of the cavity.

Table 3. Cavity performance parameters (simulated results) of the HLS-II LFB kicker with transition beam pipes (round to octagonal).

parameter	value
central frequency $f_{\rm cf}$/MHz	969.2
bandwidth BW/MHz	102.8
shunt impedance $R_{\rm s}/\Omega$	1684
quality factor Q	9.4
R/Q factor/Ω	89.6
filling time τ/ns	3.01
transit time factor T	0.835

5 Conclusion

During the design of the LFB kicker for the HLS-Ⅱ storage ring, three methods are applied to optimize the kicker performances. The nose cones are used successfully to increase the shunt impedance of the kicker cavity. The analysis based on the cavity perturbation method also shows that the nose cones can somewhat lower the resonant frequency of the kicker. The dependency calculation is a good way to allow us to produce a preliminary design of an LFB kicker starting from some known cavity designs. And finally the Newton's method is used to bring the kicker cavity performance precisely back to the design goals for the final cavity design with complex transition beam pipes without rotational symmetry. With this staged development strategy we have completed the physics design of a broadband and high shunt impedance kicker cavity with the desirable central frequency for the HLS-Ⅱ longitudinal feedback system. We have reached and in some aspects surpassed the design specifications. In fact the realized shunt impedance of 1684 Ω ($BW=102.8$ MHz) is 10% higher than that of the Duke LFB kicker ($BW=92$ MHz), representing a further optimization of the kicker cavity design, compared with the Duke LFB kicker which is a high performance cavity.

References

1 WANG Lin, LI Wei-Min, FENG Guang-Yao, XU Hong-Liang, ZHANG Shan-Cai, GAO Wei-Wei, FAN Wei. The Upgrade Project of Hefei Light Source (HLS). In Proceedings of the IPAC'10. Kyto, Japan. 2588–2590

2 Serio M, Boni R, Drago A, Gallo A, Ghigo A, Marcellini F, Migliorati M, Zobov M, Claus R, Fox J, et al. Multi-Bunch Instabilities and Cures. In Proc. European Particle Accelerator Conference. 1996

3 Oxoby G, Claus R, Fox J, Hindi H, Hoejlich J, Linscott I, Olsen J, Perbhakal S, Sapozhnikov L, Corlett J, et al. Bunch-by-Bunch Longitudinal Feedback System for PEP-Ⅱ. In EPAC 94: proceedings. 1994, 1616–1618

4 Teytelman D, Rivetta C, Van Winkle D, Akre R, Fox J, Krasnykh A, Drago A, Flanagan J, Naito T, Tobiyama M. Design and Testing of Gproto Bunch-by-Bunch Signal Processor. TH-PCH103, EPAC. 2006, 6

5 XU W, WU W, HE D, WU Y K. Design of Longitudinal Feedback Kicker for HLS Storage Ring. In Particle Accelerator Conference. New York, NY, USA, IEEE. 2011

6 Gallo A, Boni R, Ghigo A, Marcellini F, Serio M, Zobov M. A Waveguide Overloaded Cavity as Longitudinal Kicker for the DAΦNE Bunch-by-Bunch Feedback System. Part. Accel., 1996, **52**: 95–113

7 Kim Y, Kwon M, Huang J, Namkung W, Ko I. Longitudinal Feedback System Kicker for the PLS Storage Ring. Nuclear Science, IEEE Transactions on, 2000, **47**(2): 452–467

8 WU W, Kim Y, LI J, Teytelman D, Busch M,d WANG P, Swift G, Park I, Ko I. Development of a Bunch-by-Bunch Longitudinal Feedback System with a Wide Dynamic Range for the HIGS Facility. Nuclear Instruments & Methods in Physics Research. Section A. Accelerators, Spectrometers, Detectors, and Associated Equipment, 2011, **632**(1): 32–42

9 Wiedemann H. Particle Accelerator Physics. Vol. 1. Springer Verlag, 2003

10 Pozer D. Microwave Engineering. John Wiley & Sons, 2005. 298–302

11 Cohn S. Properties of Ridge Wave Guide. Proceedings of the IRE, 1947, **35**(8): 783–788

12 Kelley C. Solving Nonlinear Equations with Newton's Method. Vol. 1. Society for Industrial Mathematics, 2003